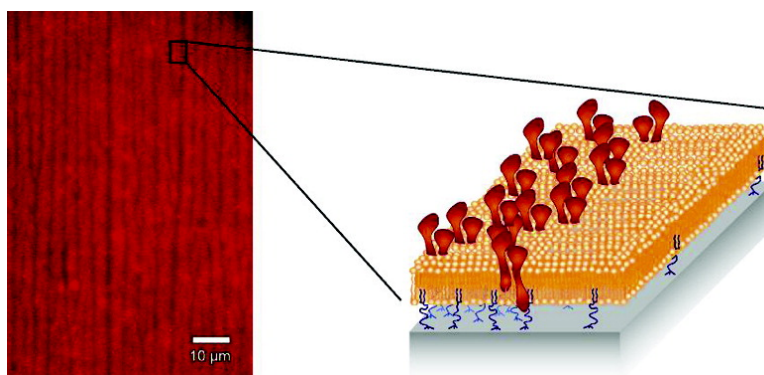


## Confinement of Transmembrane Cell Receptors in Tunable Stripe Micropatterns

Oliver Purrucker, Anton Frtig, Karin Ldtke, Rainer Jordan, and Motomu Tanaka

*J. Am. Chem. Soc.*, **2005**, 127 (4), 1258-1264 • DOI: 10.1021/ja045713m • Publication Date (Web): 08 January 2005

Downloaded from <http://pubs.acs.org> on March 24, 2009



### More About This Article

Additional resources and features associated with this article are available within the HTML version:

- Supporting Information
- Links to the 14 articles that cite this article, as of the time of this article download
- Access to high resolution figures
- Links to articles and content related to this article
- Copyright permission to reproduce figures and/or text from this article

[View the Full Text HTML](#)

## Confinement of Transmembrane Cell Receptors in Tunable Stripe Micropatterns

Oliver Purrucker,<sup>†</sup> Anton Förtig,<sup>‡</sup> Karin Lüdtker,<sup>‡</sup> Rainer Jordan,<sup>\*,†,§</sup> and Motomu Tanaka<sup>\*,†</sup>

Contribution from the Lehrstuhl für Biophysik E22, Technische Universität München, James-Franck-Strasse, 85748 Garching, Germany, Lehrstuhl für Makromolekulare Stoffe, Technische Universität München, Lichtenbergstrasse 4, 85748 Garching, Germany, and Department of Chemistry, Chemical Engineering and Material Science, Polytechnic University, Six Metrotech Center, Brooklyn, New York 11201

Received July 16, 2004; E-mail: rainer.jordan@ch.tum.de; mtanaka@ph.tum.de

**Abstract:** We report a simple method to confine transmembrane cell receptors in stripe micropatterns of a lipid/lipopolymer monolayer, which are formed as result of the transfer onto a solid substrate. The stripes are aligned perpendicular to the meniscus, whose periodicity can systematically be tuned by the transfer velocity. This strongly suggests the dominant role of the cooperative interaction between the film and substrate. Selective fluorescence labeling of lipids and lipopolymers confirms that the observed patterns coincide with the demixing of two species. Covalent coupling of polymer headgroups enables us to use the stripe patterns as a support for a lipid bilayer membrane. Spreading of lipid vesicles with platelet integrin  $\alpha_{IIb}\beta_3$  on a self-assembled membrane micropattern demonstrates that cell adhesion receptors are selectively incorporated into the lipopolymer-rich region. The method established here provides us with a tunable template for the confinement of receptor proteins to geometrically control the cell adhesion.

### Introduction

Dissipative molecular aggregates in organic materials are drawing increasing attentions as mesoscopic (or nanoscopic) compartments for the confinement of chemical functionalities.<sup>1–4</sup> Along this line, many studies have demonstrated the formation of dissipative structures in free-standing and solid-supported polymer thin films.<sup>5–7</sup> Several groups also reported stripe-like micropattern formation in transferred surfactant films, which can be categorized into two types. The first type is based on stripe-like “defects” found in lipid monolayers prepared near  $pK_a$ , or those transferred near the phase transition from the liquid-expanded (LE) to liquid-condensed (LC) phase. The pattern formation mechanism is explained as periodic oscillations of the contact angle and meniscus height of the water subphase on the substrate during the Langmuir–Blodgett (LB) transfer of the films.<sup>1,4,8–11</sup> These dewetting patterns aligned parallel to

the meniscus are interpreted in terms of substrate-mediated condensation at the three-phase contact line. By filling the periodically separated gaps with organic and inorganic filling materials, these channels show a potential application in lithographic templates.<sup>2,12</sup> More recently, Pignataro et al. reported that a lipid monolayer in LC phase forms periodic defects perpendicular to the meniscus, when the film is transferred at low temperature.<sup>13</sup> The obtained patterns suggest a different mechanism of pattern formation; however, further physical characterizations seem to be necessary to determine the dominant physical parameter. The second family of stripe micropatterns can be found in LB films of lipid mixtures, which have a clear hydrophobic mismatch.<sup>14,15</sup> In contrast to the periodic defects, the stripe patterns are topographically defined with a height difference corresponding to the mismatch in the alkyl layer thickness. Moraille recently reported the formation of a striped bilayer, suggesting the applications as a template in molecular deposition.<sup>16</sup> However, the application of such quasi two-dimensional stripe patterns for confinement of membrane associated proteins is still missing.

In the present paper, we describe a simple method to confine cell adhesion receptors in stripe micropatterns formed in mixed

<sup>†</sup> Lehrstuhl für Biophysik E22, Technische Universität München.

<sup>‡</sup> Lehrstuhl für Makromolekulare Stoffe, Technische Universität München.

<sup>§</sup> Polytechnic University.

- Gleiche, M.; Chi, L. F.; Fuchs, H. *Nature* **2000**, *403*, 173–175.
- Lenhert, S.; Zhang, L.; Mueller, J.; Wiesmann, H. P.; G. E.; Fuchs, H.; Chi, L. F. *Adv. Mater.* **2004**, *16*, 619–624.
- Shimomura, M.; Sawadaishi, T. *Curr. Opin. Colloid Interface Sci.* **2001**, *6*, 11–16.
- Moraille, P.; Badia, A. *Angew. Chem., Int. Ed. Engl.* **2002**, *41*, 4303–4306.
- Reiter, G. *Phys. Rev. Lett.* **1992**, *68*, 75–78.
- Koneripalli, N.; Levicky, R.; Bates, F. S.; Anknor, J.; Kaiser, H.; Satija, S. K. *Langmuir* **1996**, *12*, 6681–6690.
- Herminghaus, S.; Jacobs, K.; Mecke, K.; Bischof, J.; Fery, A.; Ibn-Elhaj, M.; Schlogowski, S. *Science* **1998**, *282*, 916–919.
- Spratte, K.; Chi, L. F.; Riegler, H. *Europhys. Lett.* **1994**, *25*, 211–217.
- Kovalchuk, V. I.; Bondarenko, M. P.; Zholkovskiy, E. K.; Vollhardt, D. J. *Phys. Chem. B* **2003**, *107*, 3486–3495.
- Yaminski, V.; Nylander, T.; Ninham, B. *Langmuir* **1997**, *13*, 1746–1757.

- Mahnke, J.; Vollhardt, D.; Stöckelhuber, K. W.; Meine, K.; Schulze, H. J. *Langmuir* **1999**, *15*, 8220–8224.
- Lu, N.; Gleiche, M.; Zheng, J.; Lenhert, S.; Xu, B.; Chi, L. F.; Fuchs, H. *Adv. Mater.* **2002**, *14*, 1812–1815.
- Pignataro, B.; Sardone, L.; Marletta, G. *Mater. Sci. Eng. C* **2002**, *22*, 177–181.
- Moraille, P.; Badia, A. *Langmuir* **2002**, *18*, 4414–4419.
- Solletti, J. M.; Botreau, M.; Sommer, F.; Duc, T. M.; Celio, M. R. *J. Vac. Sci. Technol. B* **1996**, *14*, 1492–1497.
- Moraille, P.; Badia, A. *Langmuir* **2003**, *19*, 8041–8049.

monolayers of lipids and lipopolymers. In the first part, we focus on characterization of the stripe patterns to determine the physical parameters that dominate the pattern formation. The stripes are aligned perpendicular to the meniscus (and thus parallel to the transfer direction), whose spacing are flexibly tunable by the velocity of the film transfer. All the individual stripes, with a spatial distance in the  $\mu\text{m}$  range, are found to be continuous up to cm length scale, and cover the entire substrate without notable defects. Selective fluorescence labeling of lipids and lipopolymers verifies that the dynamic phase separation of lipids and lipopolymers through the transfer results in the formation of microstripes. In the second part, we utilize the striped lipid/lipopolymer monolayers as a selective template to confine transmembrane cell receptors. In contrast to other physisorbed stripe-like patterns of surfactants,<sup>2,16</sup> covalent coupling of polymer headgroups can stabilize the micropatterns in water. As hydrated polymer supports can provide a thick water reservoir between the substrate and membrane,<sup>17–19</sup> human platelet integrin  $\alpha_{\text{IIb}}\beta_3$  can be incorporated preferably into the lipopolymer-rich region.

## Experimental Section

**Materials.** 1-Stearoyl-2-oleoyl-*sn*-glycero-3-phosphocholine (SOPC), 1,2-diphytanoyl-*sn*-glycero-3-phosphocholine (DPhPC), and 1,2-dimyristoyl-*sn*-glycero-3-phosphoethanolamine-*N*-(7-nitro-1-1,3-benzoxadiazol-4-yl) (NBD-PE) were purchased from Avanti Polar Lipids (Alabaster, USA), and 1,2-dihexadecanoyl-*sn*-glycero-3-phosphoethanolamine triethylammonium salt (Texas Red-PE) was from Molecular Probes (Leiden, Netherlands). Freshly distilled and deionized water (Millipore, Molsheim, R > 18 M $\Omega$ cm) was used as subphase of the LB trough.

Glass cover slides (24 × 24 mm) from Karl Hecht KG (Sondheim, Germany) were used as solid supports. Prior to the film deposition, they were cleaned in the following manner: after rinsing with acetone and methanol, the samples were immersed into a solution of 1:1.5 (v/v) H<sub>2</sub>O<sub>2</sub> (30%):NH<sub>4</sub>OH (30%):H<sub>2</sub>O for 5 min under ultrasonication, and soaked for another 30 min at 60 °C.<sup>20</sup> Finally, they were rinsed intensively with water, dried at 70 °C, and stored in sealed glass boxes.

For the preparation of lipid vesicles containing integrin, the following materials were used: Triton X-100 was purchased from Aldrich, Bio-Beads SM2 adsorbents from Bio-Rad Laboratories (Hercules), and 1-stearoyl-2-oleoyl-*sn*-glycero-3-phosphocholine (SOPC) and 1-stearoyl-2-oleoyl-*sn*-glycero-3-[phospho-*rac*-(1-glycerol)] (SOPG) from Avanti Polar Lipids. Integrins were labeled with 5-(and-6)-carboxytetramethylrhodamine, succinimidyl ester (5(6)-TAMRA-SE), purchased from Molecular Probes. Buffer solutions were prepared with tris-(hydroxymethyl)-aminomethane (Tris), purchased from Roth GmbH (Karlsruhe, Germany).

All the other chemicals were purchased from Sigma-Aldrich (Munich, Germany) and used without further purification.

**Synthesis of Silane-Functionalized Lipopolymer.** The polymerization and purification of lipopolymers followed our previous accounts.<sup>19,21,22</sup> For poly(2-methyl-2-oxazoline) lipopolymers ( $n = 104$ ) with a distearoyl lipid moiety and a trimethoxysilane anchoring group (DS-PMOX<sub>104</sub>-Si), a monomer to initiator ratio of 100:1 was adjusted, and the polymerization was carried out at 55 °C for 15 days (yield =

85%;  $\overline{DP}_{\text{NMR}} = 104$ ;  $\text{PDI}_{\text{GPC(DMAc)}} = 1.30$ ). 1,2-Di-*O*-phytanoyl-glycerol was used as initiator for DPh-PMOX<sub>21</sub>-Si (with a diphytanoyl instead of a distearoyl lipid moiety) (yield = 89%;  $\overline{DP}_{\text{NMR}} = 21$ ;  $\text{PDI}_{\text{GPC(Chloroform)}} = 1.07$ ). The DS-PMOX<sub>13</sub>-TRITC (including a fluorescent label instead of a silane coupling group) was polymerized analogue to the other lipopolymers. Here, the reaction was quantitatively terminated with piperazine to have a secondary amine function (yield = 90%;  $\overline{DP}_{\text{NMR}} = 13$ ;  $\text{PDI}_{\text{GPC(Chloroform)}} = 1.05$ ), which was functionalized with tetramethylrhodamine-isothiocyanate (TRITC), following the synthesis described in a recent account.<sup>23</sup>

**Langmuir-Blodgett Deposition of Lipid/Lipopolymer Monolayers.** Before spreading of the monolayer onto the air/water interface of a self-built Langmuir trough (subphase area: 1008 cm<sup>2</sup>), the cleaned, hydrophilic substrates were immersed into the subphase. A 70  $\mu\text{L}$  portion of an appropriate mixture of lipid and lipopolymer (dissolved in chloroform at a concentration of  $\sim 1.5 \text{ mg mL}^{-1}$ ) was spread onto the subphase. After evaporation of the solvent ( $\sim 5$ – $10 \text{ min}$ ), the film was asymmetrically compressed to a lateral pressure of  $\Pi = 30 \text{ mN m}^{-1}$  at a barrier speed of  $50 \mu\text{m s}^{-1}$  (corresponding to  $0.58 \text{ A}^2 \text{ molecule}^{-1} \text{ min}^{-1}$ ) at 20 °C. While keeping the surface pressure constant, the film was transferred onto the cleaned glass substrates at various transfer velocities ( $\sim 50$ – $500 \mu\text{m s}^{-1}$ ). The transfer ratio (the ratio between the substrate area and the decrease in the subphase area) of 1:1 verified the successful transfer of the monolayer.

**Fluorescence Microscopy.** For fluorescence studies, an inverted microscope (Axiovert 200), equipped with a 63x long distance objective (n.a. 0.75) and standard fluorescence filter sets, was used (Carl Zeiss, Göttingen, Germany). Images and movies were taken by a cooled CCD camera (Orca ER, Hamamatsu Photonics, Herrsching, Germany), digitized by a frame-grabber card (Stemmer Imaging, Puchheim, Germany), and processed by a homemade imaging software.<sup>24</sup> A Langmuir film balance (KSV Instruments, Helsinki, Finland) was coupled to the same microscope for investigation of mixed lipid/lipopolymer monolayer at the air/water interface. There, a 20x long distance objective (n.a. 0.4) was used (Carl Zeiss, Göttingen, Germany).

**Incorporation of Transmembrane Cell Receptor Integrin  $\alpha_{\text{IIb}}\beta_3$ .** The incorporation of transmembrane cell receptor integrin  $\alpha_{\text{IIb}}\beta_3$  was carried out by spreading of proteoliposomes onto the dry, hydrophobic LB monolayers, following the protocols reported previously,<sup>19,25,26</sup> and incubated for 1 h at 40 °C. The supernatant solution was removed by intensive rinsing with buffer solution, containing 20 mM Tris, 150 mM NaCl, 1 mM CaCl<sub>2</sub>, 1 mM MgCl<sub>2</sub>, and 1 mM Na<sub>2</sub>S<sub>2</sub>O<sub>3</sub> (pH 7.4).

The proteoliposomes were prepared according to the method described elsewhere:<sup>27–29</sup> Integrin  $\alpha_{\text{IIb}}\beta_3$  was extracted from human blood platelets using Triton X-100,<sup>30</sup> whose specific function was checked by enzyme-linked immunosorbent assay (ELISA) tests. For reconstitution of integrins into lipid vesicles, Triton X-100 was removed by Bio-Beads SM2. As matrix lipids, a 1:1 mixture (molar) of SOPC and SOPG was used. The integrin containing vesicles were dialyzed to 20 mM Tris, 150 mM NaCl, 1 mM CaCl<sub>2</sub>, 1 mM MgCl<sub>2</sub>, 1 mM Na<sub>2</sub>S<sub>2</sub>O<sub>3</sub> (pH = 7.4). For fluorescence microscopy, integrins were labeled with 5(6)-TAMRA-SE, whose labeling efficiency was quantified to be 100%.<sup>28</sup> The labeled and unlabeled proteins were mixed to yield a final

(17) Sackmann, E.; Tanaka, M. *Trends Biotechnol.* **2000**, *18*, 58–64.

(18) Gönnerwein, S.; Tanaka, M.; Hu, B.; Moroder, L.; Sackmann, E. *Biophys. J.* **2003**, *85*, 846–855.

(19) Purucker, O.; Förting, A.; Jordan, R.; Tanaka, M. *ChemPhysChem* **2004**, *5*, 327–335.

(20) Kern, W.; Puotinen, D. A. *RCA Review* **1970**, *31*, 187–206.

(21) Förting, A.; Jordan, R.; Purucker, O.; Tanaka, M. *Polym. Prepr.* **2003**, *44*, 850–851.

(22) Jordan, R.; Martin, K.; Räder, H. J.; Unger, K. K. *Macromolecules* **2001**, *34*, 8858–8865.

(23) Bonné, T.; Lüdtkke, K.; Jordan, R.; Štěpánek, P.; Papadakis, C. M. *Colloid Polym. Sci.* **2004**, *282*, 833–843.

(24) Keller, M.; Schilling, J.; Sackmann, E. *Rev. Sci. Instrum.* **2001**, *72*, 3626–3634.

(25) Kalb, E.; Frey, S.; Tamm, L. K. *Biochim. Biophys. Acta* **1992**, *1103*, 307–316.

(26) Plant, A. L. *Langmuir* **1993**, *9*, 2764–2767.

(27) Erb, E.-M.; Tangemann, K.; Bohrmann, B.; Müller, B.; Engel, J. *Biochemistry* **1997**, *36*, 7395–7402.

(28) Hu, B.; Finsinger, D.; Peter, K.; Guttenberg, Z.; Bärman, M.; Kessler, H.; Escherich, A.; Moroder, L.; Böhm, J.; Baumeister, W.; Sui, S.; Sackmann, E. *Biochemistry* **2000**, *39*, 12284–12294.

(29) Müller, B.; Zerwes, H.-G.; Tangemann, K.; Peter, J.; Engel, J. *J. Biol. Chem.* **1993**, *268*, 6800–6808.

(30) Fitzgerald, L.; Leung, B.; Phillips, D. *Anal. Biochem.* **1985**, *151*, 169–177.

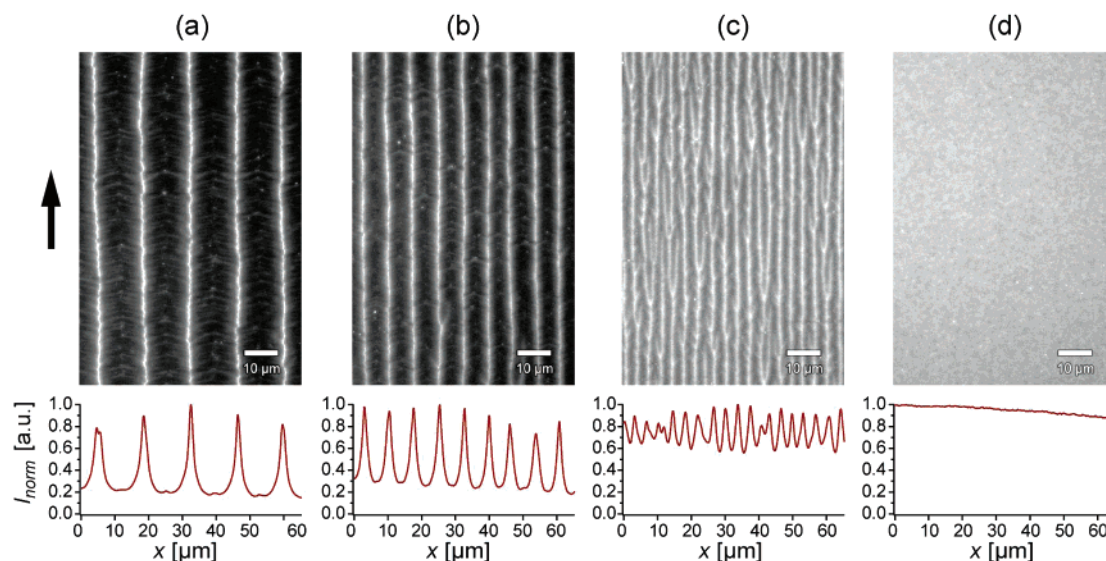


**Figure 1.** Upper row: representative fluorescence images of lipid/lipopolymer monolayers on an arbitrary position, containing 94.8 mol % SOPC, 5 mol % DS-PMO<sub>x14</sub>-Si, and 0.2 mol % Texas Red-PE. The monolayers were transferred at velocities of (a) 50, (b) 80, (c) 180, and (d) 500  $\mu\text{m s}^{-1}$ . The arrow denotes the direction of film transfer. Lower row: plots of the normalized fluorescence intensity,  $I_{\text{norm}}$ , of the horizontal cross section, averaged vertically over the whole image.

molar fraction of labeled proteins of 10%. The concentrations of proteins and lipids were determined according to the method of Bradford<sup>31</sup> and Bartlett,<sup>32</sup> respectively, yielding the molar ratio of integrin to lipid of 1:6200.

## Results and Discussion

**Influence of Transfer Velocity.** Figure 1 represents the fluorescence images (upper row) and the normalized fluorescence intensity (lower row) of the stripe micropatterns formed in lipid (SOPC)/lipopolymer (DS-PMO<sub>x14</sub>-Si) monolayers doped with 0.2 mol % of Texas Red-PE, deposited at 50, 80, 180, and 500  $\mu\text{m s}^{-1}$ . Prior to the LB transfer, fluorescence film balance experiments confirm that the lipids and lipopolymers are homogeneously mixed at the air/water interface, showing no phase separation up to  $\Pi = 40 \text{ mN m}^{-1}$  (image not shown). After the deposition onto a glass slide, stripe micropatterns parallel to the transfer direction (as indicated by an arrow) were observed. By increasing the transfer velocity from 50  $\mu\text{m s}^{-1}$  (Figure 1a) to 80  $\mu\text{m s}^{-1}$  (Figure 1b), the mean distance between individual stripes decreases:  $d_{\text{space}} = 13.7 \mu\text{m}$  (50  $\mu\text{m s}^{-1}$ ) and 7.2  $\mu\text{m}$  (80  $\mu\text{m s}^{-1}$ ). Further increase in the transfer velocity (180  $\mu\text{m s}^{-1}$ , Figure 1c) leads to a branching of stripe patterns and a decrease in the mean distance between the stripes ( $d_{\text{space}} = 3.4 \mu\text{m}$ ). At the maximum transfer velocity of our setup (500  $\mu\text{m s}^{-1}$ , Figure 1d), the structures totally vanish up to optical resolution, resulting in a homogeneous fluorescence image. It should be noted that the transfer ratio of the film, i.e., the decrease in the subphase area divided by the area of the substrate, remains 100% within the experimental error ( $\pm 5\%$ ), confirming that there is no loss of material through the transfer. Thus, the systematic dependence of the stripe periodicity on the transfer velocity strongly suggests that the self-organization of the stripe micropatterns follows the dynamic dissipation of the film in the vicinity of the three phase contact line.

**Influence of Interlayer Viscosity.** A clear tendency presented in Figure 1 suggests that one of the key parameters that also

dominates the dissipation of the film is the viscosity of the thin hydrated layer between the film and substrate, including poly(oxazoline) chains and the subphase liquid. In the vicinity of the three phase contact line, the length of poly(oxazoline) chains strongly affects the viscosity of the thin interlayer, owing to the increase in the volume fraction of polymer chains. First, we studied the influence of the polymer chain length on the stripe pattern formation. Figures 2a–c present the fluorescence images of the transferred monolayers containing 5 mol % of lipopolymers with different monomer numbers,  $n = 14, 33,$  and 104, respectively. Since the other preparation conditions are set constant (i.e., the transfer velocity of 50  $\mu\text{m s}^{-1}$  and the transfer pressure of 30  $\text{mN m}^{-1}$ ), the most dominant parameter that controls the dynamics of film dissipation is the frictional coupling between the film and the substrate. As seen in the figures, the increase in the polymer chain length leads to the transformation of *individual* stripes (DS-PMO<sub>x14</sub>-Si, Figure 2a) into *branched* stripes (DS-PMO<sub>x33</sub>-Si, Figure 2b), which further results in the reduced contrast in the fluorescence intensity (DS-PMO<sub>x104</sub>-Si, Figure 2c). Nevertheless, it should be noted that the mean distance between the fluorescent patterns does not show a clear dependence on polymer chain length, but remains the same within the experimental error ( $d_{\text{space}} = 13.7 \mu\text{m}$  for DS-PMO<sub>x14</sub>-Si, 15.1  $\mu\text{m}$  for DS-PMO<sub>x33</sub>-Si, and 14.9  $\mu\text{m}$  for DS-PMO<sub>x104</sub>-Si). The observed tendency thus denotes that the increase in the polymer chain length (i.e., the increase in the chain viscosity) causes the branching of the stripes and reduces the pattern contrast; however, it does not influence the spacing between the neighboring stripes.

Another straightforward experiment to verify the effect of interlayer viscosity is the transfer of a film from a subphase with a viscosity other than water. By replacing the water subphase to 50/50 (wt) mixture of glycerol/water, the subphase viscosity can be increased from 1  $\text{mPa s}$  to 6.0  $\text{mPa s}$ .<sup>33</sup> When

(31) Bradford, M. M. *Anal. Biochem.* **1976**, *72*, 248–254.

(32) Bartlett, G. R. *J. Biol. Chem.* **1959**, *234*, 466–468.

(33) Wohlfarth, C.; Wohlfarth, B. Viscosity of Pure Organic Liquids and Binary Liquid Mixtures. In *Landolt-Börnstein – Numerical Data and Functional Relationships in Science and Technology – New Series*; Martienssen, W., Ed.; Springer-Verlag: Berlin, 2001; Vol. IV/18A, pp 263–266.

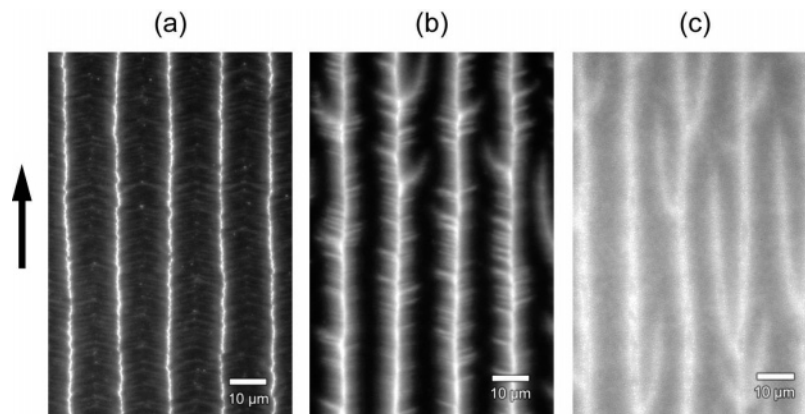


**Figure 2.** Fluorescence images of mixed monolayers containing lipopolymers with different degrees of polymerization, (a)  $n = 14$  (DS-PMOX<sub>14</sub>-Si), (b)  $n = 33$  (DS-PMOX<sub>33</sub>-Si), and (c)  $n = 104$  (DS-PMOX<sub>104</sub>-Si). The molar fraction of lipopolymer (5 mol %), the transfer pressure ( $30 \text{ mN m}^{-1}$ ), and the transfer velocity ( $50 \mu\text{m s}^{-1}$ ) were set constant in order to highlight the influence of the length of polymer chains on the stripe micropatterns. The arrow denotes the direction of film transfer.

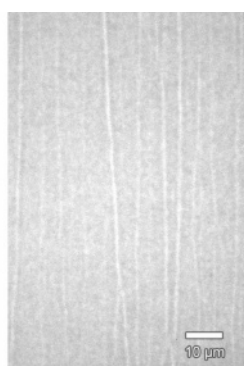


**Figure 3.** Representative fluorescence image of lipid/lipopolymer monolayers (94.8 mol % SOPC, 5 mol % DS-PMOX<sub>14</sub>-Si, and 0.2 mol % Texas Red-PE) transferred from a more viscous subphase. 50/50 (wt) glycerol/water mixture used here has a viscosity of  $6.0 \text{ mPa s}$ , which is 6 times larger than that of water. The other preparation conditions were identical to those in Figure 2.

the monolayer with the same composition as in Figure 1 is transferred from the viscous glycerol/water subphase at  $v \sim 50 \mu\text{m s}^{-1}$  (the same velocity as in Figure 1a), stripe micropatterns almost vanished (Figure 3). In fact, if the film is transferred at  $v \sim 180 \mu\text{m s}^{-1}$  (the same as in Figure 1c), no stripe micropattern can be observed within the optical resolution (data not shown).

**Influence of Hydrophobic Mismatch.** Since most of the previous accounts claimed that the packing fluctuation and phase separation of alkyl chains are responsible for the pattern formation,<sup>8,14,15</sup> we prepare a monolayer that consists of lipopolymers and lipids with diphtanoyl chains (DPh-PMOX<sub>21</sub>-Si and DPhPC). As phytanoyl chains are known to have no chain melting transition between  $T = -120$  and  $+80 \text{ }^\circ\text{C}$ ,<sup>34</sup> we can omit the possibility for the phase separation of alkyl chains due to the hydrophobic mismatch. As shown in Figure 4, the monolayer transferred at the same conditions (i.e., the transfer velocity of  $50 \mu\text{m s}^{-1}$  and the transfer pressure of  $30 \text{ mN m}^{-1}$ ) forms almost an identical stripe micropattern as those presented in Figure 2. Although the contrast in fluorescence intensity and the branching of the stripes seem slightly different, the characteristic distance between the neighboring stripes remains in the same order ( $13.5 \mu\text{m}$ ). Therefore, we can exclude the

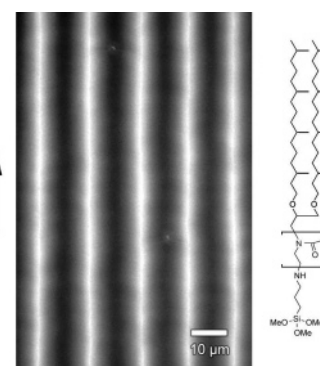


**Figure 4.** Fluorescence image of a lipid/lipopolymer monolayer containing 94.8 mol % DPhPC, 0.2 mol % Texas Red-PE, and 5 mol % DPh-PMOX<sub>21</sub>-Si. The monolayer was prepared at the same conditions as those in Figure 2. The arrow denotes the direction of film transfer.

possibility that the pattern formation is caused by phase separation of alkyl chains. The possible contribution of polymerizable trimethoxy groups on the phase separation was also examined by taking a lipopolymer with piperidine terminus. Although the lipopolymer possesses only one phytanoyl lipid anchor, we observed similar stripe patterns, verifying the negligible contribution of surface coupling groups (cf. Supporting Information).

**Selective Labeling of Lipids and Lipopolymers.** To date, all the experiments have been carried out by doping of fluorescence lipids to visualize the stripe patterns. However, this does not provide us with the conclusive standing point that the observed stripe patterns coincide with the demixing of lipids and lipopolymers but not with the segregation of fluorescence lipids. To clarify this point, we prepare a monolayer doped with NBD-labeled lipids (NBD-PE) and TRITC-labeled lipopolymers (DS-PMOX<sub>13</sub>-TRITC, see Experimental Section). By using the suitable filter sets, the fluorescence signals from each label can be monitored individually at the same region of the mixed monolayer. As presented in Figure 5 (upper left and right panels), stripe-like patterns can be observed for both labels. The overlay of two images at the identical area (Figure 5, upper middle panel) exhibits the alternative stripes of lipids and lipopolymers, showing the demixing of the two species. Actually, in the averaged cross-sectional intensity profiles (Figure 5, lower panel), the maximum intensity of one label clearly matches to the minimum of the other dye. Although the

(34) Lindsey, H.; Petersen, N. O.; Chan, S. I. *Biochim. Biophys. Acta* **1979**, *555*, 147–167.

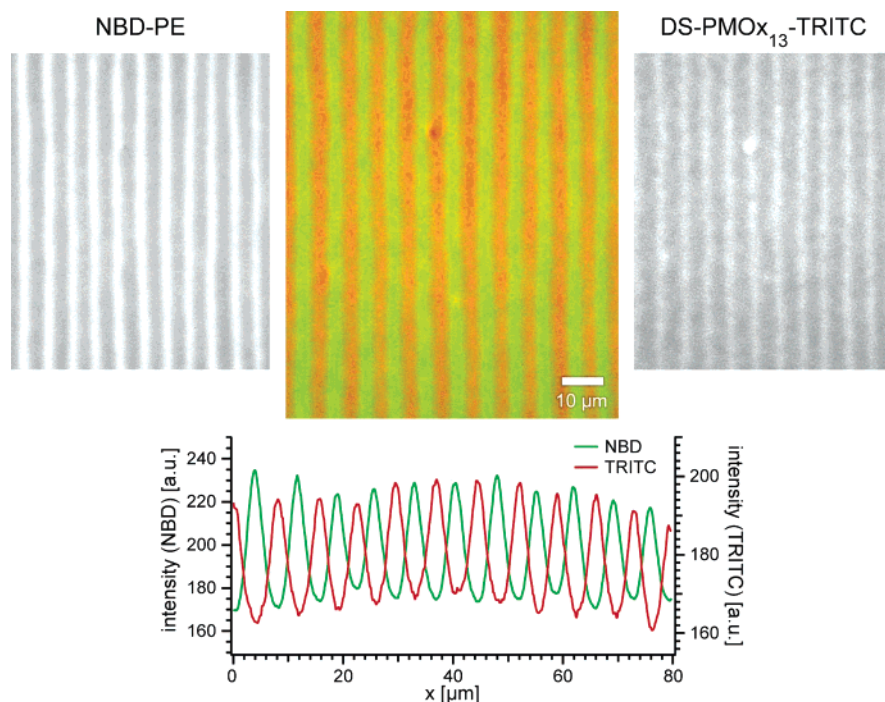


**Figure 5.** Fluorescence images of a mixed monolayer containing 0.2 mol % DS-PMO<sub>x13</sub>-TRITC, 4.8 mol % DS-PMO<sub>x18</sub>-Si, 94 mol % SOPC, and 1 mol % NBD-PE. The images from the NBD filter (upper left) and that from the TRITC filter (upper right) were taken at the same region of the monolayer. The overlay of the two images in false color (upper middle) suggests the demixing of two species, which is confirmed by the horizontal cross section of fluorescence intensities averaged vertically over the whole images (lower panel).

presented fluorescence labeling experiments do not allow us to determine if the lipids and lipopolymers are completely demixed, the selective labeling experiments indicate that a dynamic phase separation of lipids and lipopolymers results in the formation of dissipative micropatterns.

**Confinement of Cell Receptors.** Natural plasma membranes do not only possess intrinsically asymmetric distribution of lipids in their cytoplasmic and extracellular leaflets, but also form laterally organized functional microdomains enriched with certain types of lipids and proteins. These domains, known as “lipid rafts”,<sup>35</sup> are postulated to govern complex cellular functions such as endocytic traffic, signal transduction, and apoptosis. Furthermore, dynamic accumulation of ligand–receptor pairs plays an important role in cell adhesion (such as extravasation of leukocytes into tissues at inflammation sites) in order to establish a firm adhesion.<sup>36</sup> In contrast to the geometric control of cellular activities achieved by soft lithography,<sup>37</sup> we utilize here the tunable stripe patterns as self-assembled templates to confine cell receptor proteins.

In our previous accounts, we found the direct spreading of proteoliposomes onto solid substrates often causes inhomogeneous distribution of proteins due to the direct mechanical contact of proteins to a “hard” solid.<sup>18,19</sup> The homogeneity and mobility of proteins can be significantly improved by deposition of polymer supports such as thin polysaccharide films.<sup>17,18</sup> Owing to the covalent coupling of silane groups to a glass surface, the transferred lipid/lipopolymer monolayer studied here can be used as a spacer to separate a lipid membrane from the substrate. In fact, we recently found a clear influence of spacer length on the homogeneity of cell receptor proteins, platelet

integrin  $\alpha_{IIb}\beta_3$ . In contrast to an inhomogeneous distribution found for the membrane with a short spacer ( $n = 14$ ), a significant improvement in the protein distribution can be achieved by the increase of the polymer spacer length ( $n = 33$ ).<sup>19</sup> On the basis of this experimental finding, we choose here the spacer length of  $n = 33$  to selectively accommodate integrins. Indeed, when proteoliposomes with fluorescently labeled integrin  $\alpha_{IIb}\beta_3$  are incubated on a patterned monolayer consisting of 10 mol % DS-PMO<sub>x33</sub>-Si and 90 mol % SOPC, proteins are preferably incorporated into the lipopolymer-rich region (Figure 6). Although it is still not possible to quantify functions of integrins in stripe patterns, our preliminary experiments demonstrated specific interaction between synthetic ligands and the stripe patterns of integrins. As demonstrated in the first part of this study, the periodicity of the stripe patterns can be adjusted in the range of 1–10  $\mu\text{m}$ , suggesting a large potential of the tunable stripes of receptors for the control of cellular functions via geometry of protein patterns.

**Mechanism of Pattern Formation.** The stripe patterns with periodicities of  $\mu\text{m}$  range are continuous up to cm length scale, coating the entire substrate without topographic defects (cf. Supporting Information). As demonstrated in Figure 5, the stripes coincide with the demixing of lipids and lipopolymers during the film deposition. All of them are aligned perpendicular to the meniscus, whose spacing can flexibly be tuned by the transfer velocity (Figure 1). This tendency suggests the dominant role of the speed of water drainage in determination of the stripe periodicity. To adjust the frictional coupling between the surfactant headgroups (i.e., phosphocholine headgroups and polymer chains) and the solid substrate, two physical parameters are altered. The increase in the polymer viscosity as a result of the polymer chain elongation leads to the branching of the stripes and reduction in the pattern contrast (Figure 2). On the other

(35) Simons, K.; Ikonen, E. *Nature* **1997**, *387*, 569–572.

(36) Springer, T. A. *Annu. Rev. Physiol.* **1995**, *57*, 827–872.

(37) Chen, C. S.; Mrksich, M.; Huang, S.; Whitesides, G. M.; Ingber, D. E. *Science* **1997**, *276*, 1425–1428.

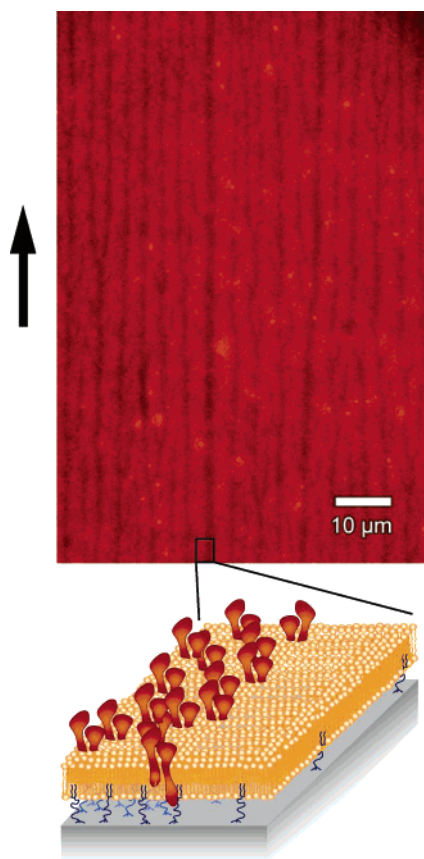


**Figure 6.** Fluorescence image of a lipid membrane containing fluorescently labeled transmembrane cell receptors integrin  $\alpha_{IIb}\beta_3$ . The proximal LB monolayer consists of 10 mol % DS-PMO<sub>x33</sub>-Si and 90 mol % SOPC, prepared at  $T = 20$  °C,  $\Pi = 30$  mN m<sup>-1</sup>, and  $v \sim 50$   $\mu\text{m s}^{-1}$ . Proteoliposomes containing labeled integrin  $\alpha_{IIb}\beta_3$  were incubated on the monolayer, resulting in the homogeneous distribution of proteins.

hand, the stripe patterns almost disappeared at an increased subphase viscosity (Figure 3). The experimental results obtained here suggest a different mechanism of the pattern formation from the other stripe defects/patterns reported previously.

For example, the striped defects aligned parallel to the meniscus in lipid monolayers are found when films are prepared near  $pK$  or transferred at the coexistence of the liquid-expanded (LE) and liquid-condensed (LC) phase.<sup>1,4,9–11,38</sup> The mechanism of pattern formation has been attributed to the fluctuation of the meniscus during the fast film transfer. Recently, Lenhert et al.<sup>2</sup> reported that the stripes aligned perpendicular to the meniscus can be formed when a phospholipid monolayer was transferred at a certain surface pressure ( $\Pi = 5$  mN m<sup>-1</sup>). However, the mechanism of pattern formation is hardly understood, although a transition from the parallel stripes to the perpendicular ones could be observed at around  $\Pi = 3.5$  mN m<sup>-1</sup>. In contrast, the mixed monolayers studied here are transferred at a high surface pressure ( $\Pi = 30$  mN m<sup>-1</sup>), corresponding to a mean area per molecule of about 50 Å<sup>2</sup>. This value suggests that the fluid alkyl chains have no free voids to create defects. In fact, tapping mode AFM experiments show no sign of topographic features (data not shown), which agrees very well with the obtained transfer ratio of  $100 \pm 5\%$ . It should be noted that the pattern formation does not depend on the crystallization of alkyl chains. The result presented in Figure 4

(38) Spratte, K.; Riegler, H. *Langmuir* **1994**, *10*, 3161–6173.

clearly excludes the possible contribution of phase separation due to hydrophobic mismatch, since the diphtanoyl chains of DPh-PMO<sub>x21</sub>-Si and DPhPC have no chain melting transition between  $T = -120$  °C and  $+80$  °C. This is in clear contrast to the recent paper by Pignataro et al.<sup>13</sup> reporting the formation of perpendicularly aligned stripe defects in a “frozen” DMPC monolayer transferred at 10 °C and  $\Pi = 30$  mN m<sup>-1</sup>. On the other hand, the other types of stripe nano-patterns were found in lipid monolayers with clear hydrophobic mismatches, i.e., the alkyl chains of two lipids are immiscible.<sup>14,15</sup> Here, the formation of the stripes aligned parallel to the meniscus are interpreted in terms of the fluctuation in molecular packing at the coexistence of lipids in LE and LC phases. This scenario does not seem to hold in our experimental systems, because the Langmuir isotherms or fluorescence film balance experiments show no sign of phase separation of lipids and lipopolymers at the air/water interface up to  $\Pi = 40$  mN m<sup>-1</sup>.<sup>19</sup> Moreover, the experiments with diphtanoyl lipid anchors (Figure 4) exclude this scenario.

At present, the exact mechanism of the pattern formation still remains unclear. The instabilities in mixtures of liquids with different viscosities and surface tensions are formed according to the concentration gradient created by evaporation of one component,<sup>39,40</sup> or by chemical reactions,<sup>41</sup> which can be referred as solutal Marangoni effects. However, the concentration of lipids and lipopolymers should be constant, since the average area per molecule and therefore, the surface tension are kept constant. This enables us to conclude that our experimental systems cannot be treated within the Marangoni-Bénard instability.

On the other hand, the successful deposition of all the films (transfer ratio of  $100 \pm 5\%$ ) confirms that the transfer velocities chosen in this study remain smaller than the maximum transfer velocity predicted by the lubrication theorem,<sup>42</sup>

$$V_{\max} \propto \frac{\gamma \theta^3}{\eta}$$

$\theta$  is the contact angle at the meniscus,  $\eta$  is the dynamic viscosity of the subphase liquid.  $\gamma$  is the surface tension ( $\gamma = \gamma_0 - \Pi$ ), corresponding to the difference between the surface tension of solvent  $\gamma$  and the surface pressure  $\Pi$  at which the deposition takes place. As experimentally demonstrated by Petrov et al.,<sup>43</sup>  $V_{\max}$  depends on the short-range intermolecular forces. The cooperative substrate-monolayer attraction can be referred as a “surface reactivity”, where the “binding energy” between the substrate and the transferred film corresponds to the energy of headgroup hydration.

As the poly(2-oxazoline) chains are hygroscopic,<sup>44</sup> one can assume a contrast in hydration forces operated within the polymer headgroups and those within phospholipids headgroups. To gain the deeper insight of the dynamic mechanism, in situ measurements of the hydrated layer thickness near the three phase contact line are necessary. One of the promising ap-

(39) Vuilleumier, R.; Ego, V.; Neltner, L.; Cazabat, A. M. *Langmuir* **1995**, *11*, 4117–4121.

(40) Fanton, X.; Cazabat, A. M. *Langmuir* **1998**, *14*, 2554–2561.

(41) Vedove, W. D.; Sanfeld, A. J. *Colloid Interface Sci.* **1981**, *84*, 318–327.

(42) De Gennes, P. G. *Colloid Polym. Sci.* **1986**, *264*, 463–465.

(43) Petrov, J. G.; Kuhn, H.; Möbius, D. *J. Colloid Interface Sci.* **1980**, *73*, 66–75.

(44) Rehfeldt, F.; Tanaka, M.; Pagnoni, L.; Jordan, R. *Langmuir* **2002**, *18*, 4908–4914.

proaches to determine the “critical” contact angle or film thickness<sup>45</sup> at which the film dissipation (or dewetting) takes place will be the combination of noninvasive imaging ellipsometry with a Langmuir film balance, which realizes nm accuracy in thickness and  $\mu\text{m}$  resolution in lateral dimensions.<sup>46</sup> Further experiments are being carried out along this line to quantify the local contact angles at the lipid-rich region as well as at the lipopolymer-rich region.

### Conclusions

Here, we report a new class of stripe micropatterns formed in transferred lipid/lipopolymer mixtures, whose spacing are tunable by several physical parameters, such as the transfer velocity and subphase viscosity. In contrast to the other stripe-like patterns of lipid monolayers, the isolated stripes with the spacing in the micrometer scale are found to be always parallel to the transfer direction in the macroscopic length scale (cm scale), exhibiting no remarkable defects. Fluorescence labeling of lipopolymer headgroups further confirmed the separation of lipids and lipopolymers through the transfer. Since the transferred lipopolymers are covalently coupled to the glass substrate,

the deposition of another lipid monolayer enables us to prepare supported lipid bilayers with defined polymer spacers.<sup>19</sup> The incubation of lipid vesicles with integrin  $\alpha_{\text{IIb}}\beta_3$  on a patterned monolayer results in preferable incorporation of proteins into the lipopolymer-rich phase. The method established here can be used for the geometrical control of cellular functions, such as cell growth, apoptosis, and cell adhesion.

**Acknowledgment.** The authors are grateful to E. Sackmann for inspiring discussions and to M. Rusp and M. Bärman for protein purification. This work was financially supported by the Deutsche Forschungsgemeinschaft (SFB 563, Ta259/5) and the Fonds der Chemischen Industrie. M.T. is thankful to the DFG for the Emmy Noether fellowship.

**Supporting Information Available:** Continuity and regularity of stripe patterns confirmed for longer length scales (Figure 1). Covalent coupling of lipopolymers confirmed by removal of physisorbed molecules with detergents (Figure 2). Influence of trimethoxy silane groups on the pattern formation, verified by piperidin termination (Figure 3). This material is available free of charge via the Internet at <http://pubs.acs.org>.

(45) Debrèges, G.; Martin, P.; Brochard-Wyart, F. *Phys. Rev. Lett.* **1995**, *75*, 3886–3889.

(46) Elender, G.; Sackmann, E. *J. Phys. II* **1994**, *4*, 455–479.

JA045713M